JCAMECH

Multi-objective optimization of geometrical parameters for constrained groove pressing of aluminium sheet using a neural network and the genetic algorithm

Sadegh Ghorbanhosseini[a],*, Faramarz Fereshteh-saniee[a]

[a] Department of Mechanical Engineering, Faculty of Engineering, Bu-Ali Sina University, Hamedan, Iran

ARTICLE INFO

ABSTRACT

One of sheet severe plastic deformation (SPD) operation, namely constrained groove pressing (CGP), is investigated here in order to specify the optimum values for geometrical variables of this process on pure aluminium sheets. With this regard, two different objective functions, i.e. the uniformity in the effective strain distribution and the necessary force per unit weight of the specimen, are selected to be minimized. To examine the effects of the sheet thickness, die groove angle and the die-tooth number on these objective functions, several finite-element (FE) analyses of the operation are carried out. Using the values of objective functions attained via these numerical simulations, an artificial neural network (ANN) is trained with good regression fitness. Employing a two-objective genetic algorithm (GA), a series of optimum conditions is obtained as a Pareto front diagram. The best optimum point in this diagram is the closest one to the origin which, at the same time, makes both the objective functions smallest. With this regard, a sheet thickness of 2 mm, a groove angle of 25° and an 8-tooth die are found to be an appropriate optimal condition for performing a CGP process. The finite-element simulation with these enhanced geometrical variables is conducted and the values of the objective functions gained from the numerical analysis is found to be in good agreement with those obtained from the genetic algorithm optimization.

1. Introduction

The severe plastic deformation is a production technique in which a fine-grained component is produced by inducing high strains into the material without changing the main dimensions of the workpiece[1]. By this means the microstructure of the part is considerably modified such that the grain size can be reduced into a nanoscale and consequently, mechanical properties of the material is significantly improved whereas the size of the component is nearly unchanged. This type of strengthening is carried out without addition of alloying elements and/or ceramic particles [2]. During past two decades, various SPD methods have been proposed by different researchers, among which the constrained groove pressing technique is employed for increasing the strength the sheet metals. A CGP operation is based on repeated corrugating and flattening of the sheet via shearing and bending applied by the press of a grooved die. A schematic illustration of this process is shown in Fig. 1. The workpiece is first bent and corrugated by means of a grooved die (Figs. 1a and 1b). Afterwards, by pressing the deformed part using a flat die, it

is plastically deformed into its initial shape (Fig. 1c). This sheet is, then, rotated 180° about the vertical axis (normal to the sheet), and the grooving and straightening operations are repeated (Figs. 1d to 1f). Redoing the forming cycle shown in Fig. 1 for several times, one can induce huge strains into the material, resulting in significant modifications in its microstructure and considerable improvement in its mechanical properties. The main advantage of the CGP process is its applicability to sheet metals.
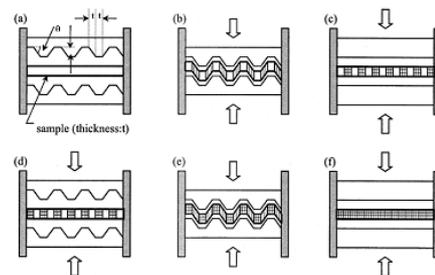
Figure 1. Different stages of a constrained groove pressing operation [3].

[1] Corresponding author. Tel.: +98 81 38292630; fax: +98 81 38292631; e-mail: s.ghorbanhosseini92@basu.ac.ir

The CGP operation was initially introduced by shin et al. [4]. They used a grooved die for pressing and applying shear deformations to a pure aluminium sheet under plane strain conditions. Using the finite element method, Lee and Park [3] numerically simulated this sort of sever plastic process. Rafizadeh et al. [5] employed this forming technique to produce fine-grained pure copper sheets. They investigated the influences of the number of forming cycles and intermediate and final annealing processes on the yield strength, microstructure and hardness of the final product. Khakbaz and Kazeminezhad produced fine-grained Al-Mn alloy sheets using CGP technique [6] and, by conducting the tensile test at various strain rates, found out that after three passes of the operation, the strain rate sensitivity of the material was increased from 0.0081 to 0.019. Borhani and Djavanroodi [7] employed a rubber pad between the workpiece and the upper die during the CGP of Al sheets. They observed that the mechanical properties such as UTS, the yield strength and hardness were significantly increased, whereas the ductility of the alloy was reduced. Kumar and Raghu [8] employed the constrained groove pressing to make fine-grained nickel sheets. Wang et al. utilized DEFORM-3D software for establishing a multi-pass CGP operation. They analyzed the influence of processing parameter such as groove width, groove angle, friction coefficient and deformation rate on distribution and homogeneity evolution of equivalent strain based on Taguchi optimization method. They found that groove angle and groove width are the two most important parameters in CGP process [9]. Siddesha and Shantharaja [10] studied on the effect of cyclic constrained groove pressing parameters on tensile properties of Al6061/Sic metal matrix composites. They used Taghuchi robust design method to determine the optimal condition for Al6061/Sic metal matrix composites. Their experimental results indicated that the number of passes and Wt. % of Sic are most influencing parameters on this goal. Fong et al. [11] conducted the CGP process on AZ31 magnesium sheets for three samples with different temperatures during various passes and observed a considerable reduction in the average grain size, namely from 13.3 μm to 1.9 μm after the forth cycle. Yang et al. [12] compared the constrained and unconstrained groove pressing processes regarding the amount of the induced effective strain, the resulted microstructure and tensile properties of 5052 Al alloy. They claimed that the mechanical properties of the product of the CGP operation were much better than those of the unconstrained process. Fracture and fatigue behaviors of AZ31 Mg alloy subjected to the CGP process were also investigated by Salvati et al. [13] and a method was developed for prediction of fatigue crack growth. Using four cycles of this SPD technique, Hajizadeh et al. [14] increased the microhardness and the yield strength of 1050 Al alloy by 62% and 95%, respectively. Lin et al. [15] tried to employ CGP at elevated temperatures for grain refinement of AZ31 Mg sheets. The mechanical and electrical properties together with the corrosion resistance of Al-Mn-Si alloy, deformed through the constrained groove pressing, were also studied by Pouraliakbar et al. [16].

Nowadays, the artificial neural network is extensively used in various fields of research. Kotkunde et al. [17] studied the significance of important process parameters, namely the punch speed, blank holder pressure and temperature on forming limit diagram of a Ti-6Al-4V alloy. Then, they predicted the values of major and minor strains by using artificial neural network. A systematic analysis of experimental data was conducted by Mandal [18] using artificial neural network and the buckling load predicted by the ANN models were compared with the corresponding experimental ones. Wakchaure et al. [19]

conducted a multi-response optimization of friction stir welding process for an optimal parametric combination to yield favourable tensile and impact strengths using the Taguchi based Grey Relational Analysis (GRA) and the artificial neural network. An artificial neural network was also used by Lakshmi et al. [20] to predict the flow stress of austenite stainless steel 304 and estimation of the mechanical properties of this steel by conducting tensile testing at superplastic forming temperatures. Yaghoubi and Fereshteh-saniee investigated effect of optimum forming parameters in hydro-mechanical deep drawing process. They conducted 27 FE simulations of the operation and trained a neural network on simulation's results. After that, by using the genetic algorithm, they obtained the optimum design parameters [21].

In order to produce a component with desired properties and high quality, determination of optimum values for different parameters of a specific forming process is essential. As explained above, most of the previous research works regarding the CGP operation were about metallurgical properties of the fine-grained sheets. For this reason, in the present investigation, by using the finite-element simulation, the influences of three geometrical variables on the required forming load and homogeneity of the product were examined. These variables are the sheet thickness, groove angle of the die and the number of groove teeth. Afterwards, an artificial neural network model was developed. This model was employed by the genetic algorithm for multi-objective optimization. Finally, the optimized conditions for the process variables were introduced as a pareto front and based on the considered objective functions.

2. Numerical simulations of the CGP process

The CGP process is numerically modelled using the ABAQUS software. These FE simulations were conducted for a complete cycle of the operation and the uniformity in the distribution of the effective strain in the deformed part as well as the necessary forming load were examined. The work sheet was 50*50*1 mm and made of pure Aluminium with a tensile stress-strain curve obtained by Sajadi et al. [22]. Material composition and mechanical properties of the given Aluminium sheet are presented in Table 1 and Table 2 respectively. The modelling was conducted three dimensionally (3D). Upper and bottom grooved dies were considered as discrete rigid parts and the workpiece was considered as a 3D deformable part. Since the CGP process is assumed as a quasi-static operation, the constant velocity of the upper die was considered to be 0.1 mm/sec. The interfacial friction coefficient was selected to be 0.1. To prevent the failure of the workpiece under simulation, the mass scaling and adaptive remeshing capabilities of the software were employed. And finally, Deformable sheet was modeled using An 8-node linear brick, reduced integration, hourglass control elements (C3D8R). Fig. 2 illustrates the position of dies and Aluminium sheet under the CGP process in the beginning of simulation.

Table 1. Material composition of pure Aluminium sheet [22].

Material	Al	Fe	Si	Ti	Cu	Zn	Ni	V	Mg
Wt. %	99.59	0.26	0.07	0.02	0.02	0.01	0.01	0.01	0.01

Table 2. Mechanical and physical properties of pure Aluminium sheet [22].

Properties	Value
Yield Stress (MPa)	53.75
Density ($\frac{Kg}{m^3}$)	2710.00
Young's Modulus (GPa)	71.00
Poisson's Ratio	0.33
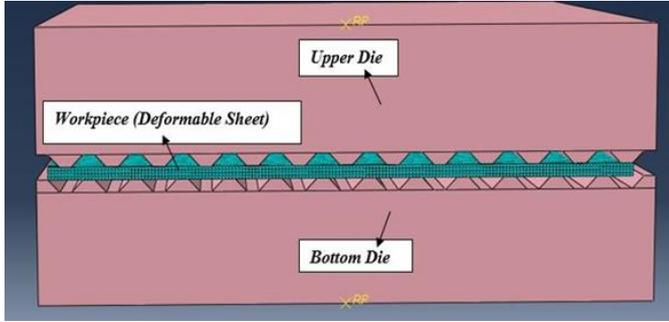
Figure 2. Finite element model of constrained groove pressing operation created in ABAQUS.

As mentioned above, the geometrical parameters of the dies of the CGP operation could significantly affect the mechanical properties of the resulting component. Some of these variables are the sheet thickness, groove angle and the number of teeth of the grooved die. All these could not only influence the forming load but also the distribution of the effective strain in the workpiece. The main objective of conducting the FE analyses was studying the effects of the above mentioned parameters on the required force and the uniformity of the deformed part. Then, by employing the artificial neural network and the genetic algorithm, it would by possible to find the optimum conditions for the process. To achieve this goal, two values were selected for the sheet thickness, namely 1mm and 2 mm. The groove angle θ (see Fig. 1) was also chosen to be 30, 45 and 60. Finally, based on the dimensions of the sheet, the number of teeth for the grooved die was adopted to be 7, 9, 11 and 13. These values for various process variables were selected based on practical considerations and those values adopted in the previous researches. Therefore, altogether 24 FE simulations were carried out in order to determine the optimized process conditions.

In the present investigation, the influences of the above geometrical parameters on the uniformity of the part have been examined. For this reason, the maximum and the average plastic effective strains of the work sheet were extracted from the FE simulations. Moreover, the maximum required forming load in each analysis was determined. These data made the necessary information for evaluation of two separate objective function. The first objective function was an indication of uniformity of the workpiece, whereas the second one involved the necessary forming load per unit weight of the component. The first objective function was defined as below:

$$OF_1 = \frac{\overline{\varepsilon}_{max} - \overline{\varepsilon}_{ave}}{\overline{\varepsilon}_{ave}} \tag{1}$$

Where $\overline{\varepsilon}_{max}$ and $\overline{\varepsilon}_{ave}$ are respectively the maximum and the average plastic effective strains induced into the work sheet. We expected the CGP process to create as high as possible plastic strains in the deformed part (i.e. a great $\overline{\varepsilon}_{ave}$). However, at the same time, we were interested in having as uniform as possible

product (i.e. a small difference between the maximum and average effective strains). Therefore, OF_1 should be minimized. The second objective function was introduced as follow:

$$OF_2 = \frac{F_{max}}{10^7 * W} \tag{2}$$

where F_{max} is the maximum force specified from the load-displacement curve of the process and W is the weight of the sheet. Coefficient 10^7 is employed to bring OF_2 into an appropriate scale (i.e. comparable with values of OF_1). In Table 3, the simulation conditions together with the corresponding results are summarized for all the 24 FE analyses. Parameters t (in mm), θ (in degree) and N respectively stand for the sheet thickness, groove angle and tooth number of the die. Various parameters such as $\overline{\varepsilon}_{max}$, $\overline{\varepsilon}_{min}$ and F_{max} were determined based on the numerical results. Using these parameters, the objective functions OF_1 and OF_2 were calculated employing Eqs. (1) and (2).

3. Optimization of CGP variables

3.1. Artificial neural network training

An artificial neural network is a composition of various units named neurons. The inputs of these neurons are first multiplied by the relevant weight factors and, then, added to a constant called the bias. Afterwards, the results pass through a non-linear function to obtain the output. The schematic of this procedure is shown in Fig.3. The number of neurons in the hidden layer of a neural network has a significant influence on the performance of the network. The appropriate selection of the number of neurons is a compromise between the generalization ability and the convergence of the network. Multi-layer neural networks are capable of selecting suitable number of layers and neural cells to perform a non-linear mapping with desired accuracy [23].

In the present investigation, three inputs (geometrical CGP die parameters) and two outputs (two objective functions) are selected. The inputs are sheet thickness (*t* in mm), the groove angle (θ in degree) and number of die teeth (N). The first output is defined based on the average and maximum effective strains induced into the workpiece. The maximum required forming load is also selected as the second output. Therefore, a couple of networks should be trained using the available data. The first one is constructed employing the three inputs and the first output. The second network is used with the same inputs but the second output (i.e. the necessary forming load). For establishing a relation between the inputs and outputs of the numerical simulations and creation of appropriate estimating function a neural network with the following characteristics is developed. A neural network with a hidden layer involving ten neurons and a tan-sigmoid transforming function together with an output layer containing 24 neurons and a linear transforming function is developed in MATLAB software for the present research work. The training of this neural network is conducted employing the Levenberg-Marquardt algorithm. With this regard, 16 data were used for training the network, 4 data were employed for testing the network and 4 data were also utilized for validation procedure, where the last group of data was randomly selected by the software during the training stage.

Table 3. The input and output parameters of the FE simulation of CGP process.

Test No	$t\,(mm)$	θ	N	ε^p_{max}	ε^p_{ave}	OF_1	$F_{max}\,(KN)$	OF_2
1	1	30	7	1.03	0.48	1.14	69	0.487
2	1	30	9	1.36	0.66	1.06	126	0.549
3	1	30	11	1.03	0.57	0.81	199	0.587
4	1	30	13	1.23	0.63	0.95	289	0.616
5	1	45	7	0.77	0.43	0.79	148	0.666
6	1	45	9	0.77	0.42	0.83	265	0.732
7	1	45	11	0.77	0.45	0.71	397	0.742
8	1	45	13	0.77	0.44	0.75	540	0.728
9	1	60	7	1.15	0.50	1.30	396	0.970
10	1	60	9	1.16	0.50	1.32	689	1.033
11	1	60	11	1.2	0.50	1.40	1070	1.082
12	1	60	13	1.46	0.47	2.11	1746	1.270
13	2	30	7	1.33	0.69	0.93	393	0.348
14	2	30	9	1.33	0.67	0.98	729	0.398
15	2	30	11	1.45	0.69	1.10	1252	0.463
16	2	30	13	1.40	0.61	1.29	1600	0.428
17	2	45	7	0.81	0.38	1.13	749	0.420
18	2	45	9	0.81	0.39	1.08	1349	0.465
19	2	45	11	0.81	0.40	1.02	2060	0.480
20	2	45	13	0.81	0.38	1.13	2950	0.495
21	2	60	7	0.85	0.46	0.84	1415	0.433
22	2	60	9	0.85	0.47	0.81	2394	0.448
23	2	60	11	0.85	0.46	0.84	2629	0.332
24	2	60	13	1.40	0.46	2.04	5278	0.480

Figure 3. The structure of an artificial neural network with input layer, output layer and hidden layers [23].

3.2. Multi-objective genetic algorithm optimization

Multi-objective optimization also known as Pareto optimization is an area of making, that is concerned with mathematical optimization problems involving more than one objective function to be optimized simultaneously. Multi-objective optimization has been applied in many fields of science, including engineering, economics and logistics where optimal decisions need to be taken in the presence of trade-offs between two or more conflicting objectives. In this paper, after construction of a desired neural network to achieve the values of the objective functions, it is possible to attain the optimized geometrical dimensions of the CGP dies by using the genetic algorithm technique. This has been carried out by programming in MATLAB software, where the initial population for creation of new generations and the crossover rate were respectively selected to be 100 and 0.7. With this regard, an evolutionary genetic algorithm is employed for multi-objective optimization purpose. As noted at the beginning of this paragraph, in a multi-objective optimization, different objective functions may be introduced that should be optimized at the same time. This functions could be in contrary to each other. In other words, the improvement of an objective function could be accompanied with degradation of the other one. This is the case in this investigation. The FE analyses showed that by decreasing the forming force (the 2nd objective function), the uniformity of the product (the 1st objective function) was increased (please see Table 3). Therefore, there is not just one solution for this optimization problem and, instead, there could be a series of optimum conditions. These are called optimum solutions or Pareto front, which are usually faced in a multi-objective optimization. None of these optimum solutions has the priority compared with the other ones, but all of them represent better results for the objective functions in comparison with non-optimum conditions [24]. Therefore, having an initial population, it is possible to create a new population. The new population could be ranked to update the Pareto front. Finally, based on the appropriateness of the results and their ranking and by using a suitable stopping criterion, the final Pareto front could be attained. The general mathematical description of this procedure is as follow. The vector $X^* = [x_1^*, x_2^*, ..., x_n^*]^T$ should be found in order to optimize the below function [24]:

$$F(X) = [f_1, ..., f_n]^T \tag{3}$$

Which involves m inequality constraints:

$$g_i(X) \leq 0, i = 1 : m \tag{4}$$

In the present research work, a couple of inequalities regarding the limitations for the number of die teeth and the groove angle are introduced as below:

$$N - 13 \leq 0; 5 - N \leq 0; \theta - 90 \leq 0; -\theta \leq 0 \tag{5}$$

Moreover the equality constraints are:

$$h_j(X) = 0, j = 1 : p \tag{6}$$

$$t - 1 = 0 \text{ or } t - 2 = 0 \tag{7}$$

Where h_j is equality constraints and t is the thickness of the workpiece in mm. In the above relationships **X** is the vector of the input variables and **F(X)** is the vector of the objective functions that should be minimized.
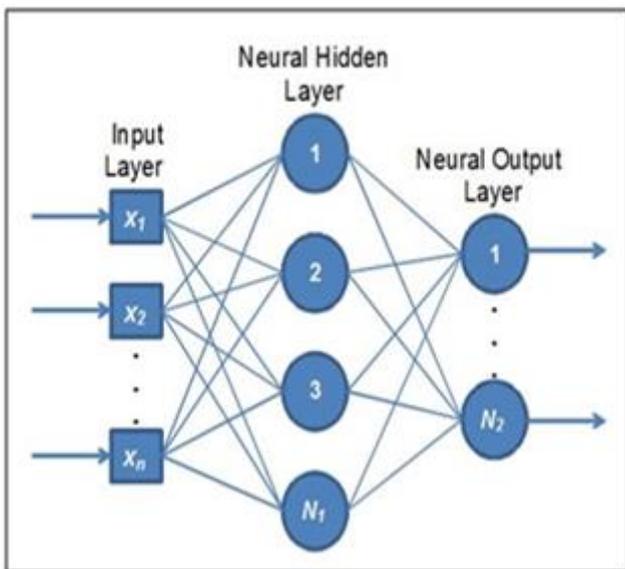
4. Results and discussions

Fig. 4 shows the deformed sheet between upper CGP die and the bottom one. As it can be seen in Fig. 4 deformed sheet filled the space between two CGP dies. Furthermore, stress distribution among sheet's elements in ABAQUS under the first stage of CGP process is shown. By getting a reference point from upper die in CGP process, magnitude of forming load and upper die stroke could be attained. These two quantity (forming load-upper die stroke) could be drawn in a graph entitled to load-displacement diagram. For validation of the numerical results, the load-displacement curve of the FE simulation of the first stage of the constrained groove pressing (i.e. the corrugation of the initial blank) was compared with the corresponding experimental one obtained by Sajadi et al. [22] (Fig.5). As shown in Fig.5, the trends of both the curves are almost the same. The forming load necessary for the first stage of a CGP process starts from zero and gradually increases with a gentle slope up to 50 KN. Afterwards, magnitude of forming load does not a significant change in the presence of upper die displacement (lower than 50 KN change in forming load versus more than 0.7 mm movement for upper die) until the material almost fill the die. And finally, since the bottom die is filled out from the workpiece, by increasing the upper die stroke less than 0.2 mm, the pressing load increases sharply to higher values until the first stage of the CGP operation is finished. In the FE simulation, for just 1 mm displacement of the die, the maximum load was about 475 KN. The difference in the final required forming loads, which in turn dictates the capacity of the hydraulic press, is quite small. However, there is a systematic overestimation in the forming load made by the FE analysis which could be due to relevant overestimations in experimental determinations of the flow curve of the material and/or the interfacial friction [22].
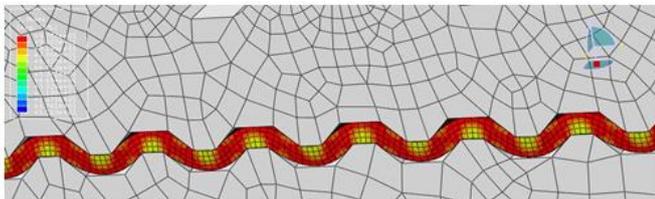
Figure 4. Schematic of a deformed sheet under CGP operation in ABAQUS.
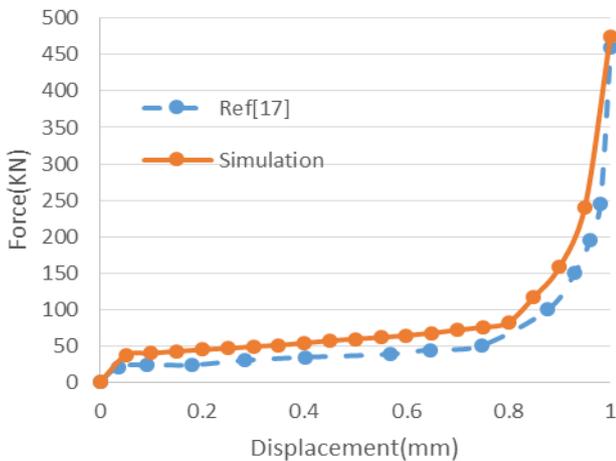
Figure 5. A comparison between the FE load-displacement curve and corresponding experimental one [22] for a typical CGP operation.

4.1. Result of ANN training

Figs.6 and 7 compare the FE data with the output of the trained ANN. Fig. 6 is related to the [1]st objective function, i.e. the uniformity in strain distribution. The maximum required loads per unit weight of the workpiece, obtained from the FE simulations and the designed ANN, are contrasted in Fig.7. In both the figures, the solid line corresponds to the ANN fitted on the numerical FE results. The dotted line is related to situations, where the output of the trained ANN exactly coincides on the corresponding FE input data. The circles also belong to the FE input data. Because of high values of fitness (R values shown in both the figures), Figs.6 and 7 imply that the constructed ANN is well trained, although the fitness for the required force is better than that of the uniformity of the product. This is mainly due to scattered nature of estimation of strain distribution compared with the load predictions by means of the FE analyses. For instance, for a specific die angle, the forming load increases by increasing the number of die teeth. Moreover, for a constant number of teeth, the necessary force increases by addition of the groove angle. Therefore, these clear trends make it possible to fit an appropriate ANN onto the data relating to the load objective function. That is why, in Fig.7, a regression fitness of 0.98472 is achieved for this objective function. However, for the uniformity objective function, a lower regression value (0.89445) is obtained because for a fixed value of a parameter, no clear and specific trend can be found for the objective function by variation of the other parameters. For example, when the number of die teeth is fixed, by increasing the groove angle from 30° to 45°, the uniformity objective function decreases. But the value of this objective function increases when the die angle is increased from 45° to 60°.
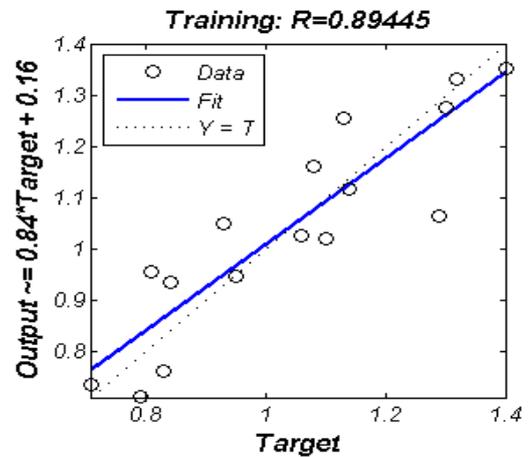
Figure 6. The finite-element and ANN data regarding the uniformity of strain distribution for the first step of the CGP operation.

Afterwards, Figs. 8 and 9 shows the comparison between FE simulations and ANN prediction of both objective functions for all 24 data series. As it can be seen in Figs. 8 and 9, most of the FE simulations and ANN prediction data matched to each other. This means that it is possible to trust these two neural networks for utilizing them to minimize the two objective functions for optimizing the CGP process.
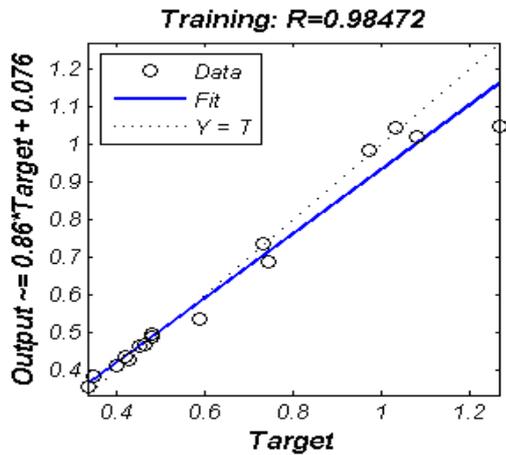
Figure 7. The finite-element and ANN data regarding the required forming load for the first step of the CGP operation.
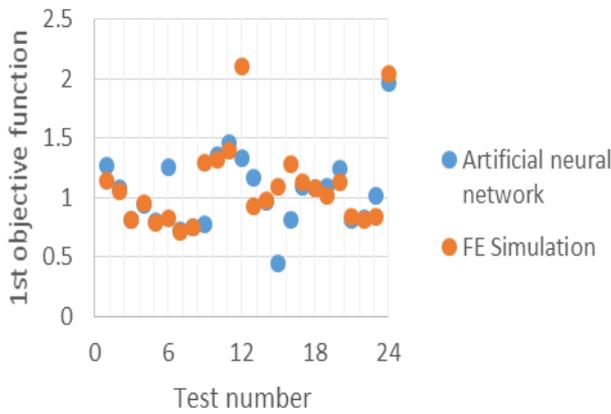
Figure 8. Comparison between FE simulation and ANN prediction for all 24 test number regarding the uniformity of strain distribution for the first stage of the CGP operation.
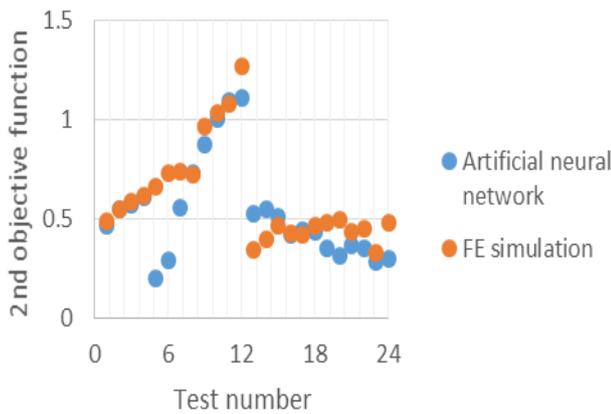
Figure 9. Comparison between FE simulation and ANN prediction for all 24 test number regarding the required forming load for the first stage of the CGP operation.

4.2. Optimum condition based on the Pareto front

Based on the selected objective functions, the Pareto front diagram for the problem under consideration is plotted in Fig.10. As can be observed in this figure, none of the optimum points in the diagram has the absolute priority with respect to the others. In

other words, each of these points can be considered as the optimum condition for introducing the optimized dimensions of the CGP dies. In Fig.10, point A corresponds to the minimum value of the first objective function (uniformity of the workpiece) but the maximum value for the second one (force per unit weight). Values of these functions were respectively 0.23 and 1.2 and the relevant optimum process could be conducted with a sheet thickness of 2 mm, a groove angle of 90° and a die with 10 teeth. In the opposite side, point C corresponds to a minimum required load (OF_2=0.53) and maximum inhomogeneity in strain distribution (OF_1=0.44). For this case the CGP operation should be performed with 1 mm thick sheet, zero groove angle and a die with 5 teeth. In Fig.10, when the priority is changed from OF_1 to OF_2, the groove angle of the die should be varied from 90° to 0°. This point is important to note that 0° and 90° groove angles are not practical for constructing a CGP die, they are presented just in order to completely cover the range of the groove angle and explain the extreme values of OF_1 and OF_2 for these die angles. It means that the input data A and C are not necessary the actual geometrical parameters for producing the final CGP die, and they are just used as the boundary solutions for the optimization problem. The groove width has also the same size as the sheet thickness. It is obvious that the thinner the workpiece, the lower is the pressing force. In Fig.10, the sheet thickness for points A and C are respectively 2 mm and 1 mm. Hence, it is reasonable that point A propose the maximum required forming load and point C represents the minimum force. Considering the geometry of the die and the workpiece in a CGP operation (Fig.1), the greater number of die teeth enlarges the size of the component and, consequently, intensifies the necessary process load. Therefore, the minimum force corresponds to the least number of teeth (N=5) which is in agreement with the Pareto front shown in Fig.10. Based on the significance of the first or the second objective function, one may respectively introduce the left or the right points of the Pareto front (Fig.10) as the optimum process conditions. However, certain compromises should be carried out with this regard. For instance, based on the design and manufacturing considerations, it seems that middle points such as point B might be more appropriate conditions for the CGP operation. Point B in Fig.10 corresponds to a sheet with a 2 mm thickness, a groove angle of 25° and an 8-tooth die. The values of OF_1 and OF_2 for these optimum process parameters are respectively 1.01 and 0.27 which are practically fair for a constrained groove pressing operation.
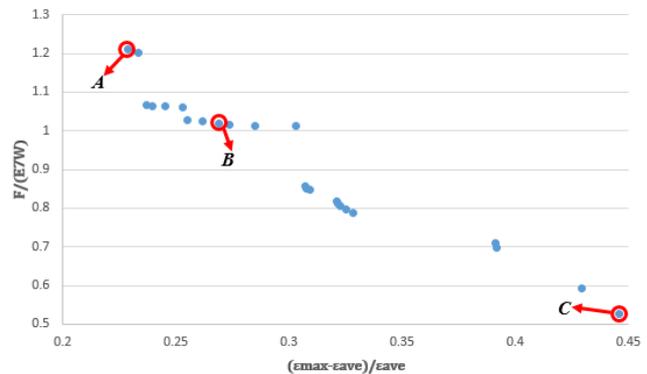
Figure 10. Pareto front based on the two objective functions.

The FE simulation of the process with these optimized variables has been conducted and the numerical values of the objective functions together with those obtained from the genetic algorithm optimization are summarized in Table 4. It is clear from Table 4 that the agreement between various results are

encouragingly good and, hence, the optimum process condition is reliable.

Table 4. A comparison between the results of the GA optimization and the FE simulation of the CGP process for point B of the Pareto front of fig.8.

Objective Function	GA Optimization	FE Simulation Based on Input Data	Error Percentage Between FE Simulation and Ga Optimization Result
OF$_1$	1.01	0.96	%5
OF$_2$	0.27	0.29	%6

5. Summary and conclusions

One of sheet severe plastic deformation processes, namely constrained groove pressing, was investigated in order to determine the optimum geometrical variables for this forming operation. Two different objective functions, i.e. the uniformity in effective strain distribution (OF$_1$) and the required force per unit weight of the workpiece (OF$_2$), were selected to be minimized. To study the influences of the sheet thickness, die groove angle and the die-tooth number on these objective functions, altogether 24 finite-element simulations of the process were conducted. Using the values of the objective functions obtained from these numerical analyses, an artificial neural network was trained with encouraging regression fitness. Finally, employing a two-objective genetic algorithm, a series of optimum process conditions was obtained as a Pareto front diagram. Depending on the priority of each objective function, each point of the Pareto front obtained could be selected as the optimum condition for the CGP operation. However, the best optimum point is the closest one to the origin of the Pareto diagram which simultaneously makes both the objective functions minimum. With this regard, a sheet thickness of 2 mm, a groove angle of 25° and an 8-tooth die were found to be a suitable optimum condition for conducting a CGP operation. The FE analysis with these optimized geometrical parameters was conducted and the values of objective functions obtained from the numerical analysis were in good agreement with those gained from the genetic algorithm optimization.

References

[1] R. Valiev, A. Korznikov, R. Mulyukov, Structure and properties of ultrafine-grained materials produced by severe plastic deformation, *Materials Science and Engineering: A,* Vol. 168, No. 2, pp. 141-148, 1993.

[2] M. J. Zehetbauer, R. Z. Valiev, 2006, *Nanomaterials by severe plastic deformation*, John Wiley & Sons,

[3] J. Lee, J. Park, Numerical and experimental investigations of constrained groove pressing and rolling for grain refinement, *Journal of Materials Processing Technology,* Vol. 130, pp. 208-213, 2002.

[4] D. H. Shin, J.-J. Park, Y.-S. Kim, K.-T. Park, Constrained groove pressing and its application to grain refinement of aluminum, *materials Science and Engineering: A,* Vol. 328, No. 1-2, pp. 98-103, 2002.

[5] E. Rafizadeh, A. Mani, M. Kazeminezhad, The effects of intermediate and post-annealing phenomena on the mechanical properties and microstructure of constrained groove pressed copper sheet, *Materials Science and Engineering: A,* Vol. 515, No. 1-2, pp. 162-168, 2009.

[6] F. Khakbaz, M. Kazeminezhad, Strain rate sensitivity and fracture behavior of severely deformed Al–Mn alloy sheets, *Materials Science and Engineering: A,* Vol. 532, pp. 26-30, 2012.

[7] M. Borhani, F. Djavanroodi, Rubber pad-constrained groove pressing process: Experimental and finite element investigation, *Materials Science and Engineering: A,* Vol. 546, pp. 1-7, 2012.

[8] S. S. Kumar, T. Raghu, Mechanical behaviour and microstructural evolution of constrained groove pressed nickel sheets, *Journal of Materials Processing Technology,* Vol. 213, No. 2, pp. 214-220, 2013.

[9] Z. S. Wang, Y. J. Guan, L. B. Song, P. Liang, Finite Element Analysis and Deformation Homogeneity Optimization of Constrained Groove Pressing, in *Proceeding of,* Trans Tech Publ, pp. 505-513.

[10] H. Siddesha, M. Shantharaja, optimization of cyclic constrained groove pressing parameters for tensile properties of Al6061/sic metal matrix composites, *Procedia Materials Science,* Vol. 5, pp. 1929-1936, 2014.

[11] K. S. Fong, M. J. Tan, B. W. Chua, D. Atsushi, Enabling wider use of Magnesium Alloys for lightweight applications by improving the formability by Groove Pressing, *Procedia CIRP,* Vol. 26, pp. 449-454, 2015.

[12] K.-h. Yang, J.-m. Zeng, W.-z. Chen, Y.-t. Huang, Influence of die construction on equivalent strain, microstructures, and tensile properties of 5052 aluminum alloy processed by groove pressing, 2016.

[13] E. Salvati, H. Zhang, K. S. Fong, R. J. Paynter, X. Song, A. M. Korsunsky, Fatigue and Fracture behaviour of AZ31b Mg alloy plastically deformed by Constrained Groove Pressing in the Presence of Overloads, *Procedia Structural Integrity,* Vol. 2, pp. 3772-3781, 2016.

[14] K. Hajizadeh, S. Ejtemaei, B. Eghbali, Microstructure, hardness homogeneity, and tensile properties of 1050 aluminum processed by constrained groove pressing, *Applied Physics A,* Vol. 123, No. 8, pp. 504, 2017.

[15] P. Lin, T. Tang, Z. Zhao, W. Wang, C. Chi, Refinement Strengthening of AZ31 Magnesium Alloy by Warm Constrained Groove Pressing, *Materials Science,* Vol. 23, No. 1, pp. 84-88, 2017.

[16] H. Pouraliakbar, M. R. Jandaghi, G. Khalaj, Constrained groove pressing and subsequent annealing of Al-Mn-Si alloy: microstructure evolutions, crystallographic transformations, mechanical properties, electrical conductivity and corrosion resistance, *Materials & Design,* Vol. 124, pp. 34-46, 2017.

[17] N. Kotkunde, A. D. Deole, A. K. Gupta, Prediction of Forming Limit Diagram for Ti-6Al-4V Alloy Using Artificial Neural Network, *Procedia materials science,* Vol. 6, pp. 341-346, 2014.

[18] P. Mandal, Artificial neural network prediction of buckling load of thin cylindrical shells under axial compression, *Engineering Structures,* Vol. 152, pp. 843-855, 2017.

[19] K. Wakchaure, A. Thakur, V. Gadakh, A. Kumar, Multi-Objective Optimization of Friction Stir Welding of Aluminium Alloy 6082-T6 Using hybrid Taguchi-Grey Relation Analysis-ANN Method, *Materials Today: Proceedings,* Vol. 5, No. 2, pp. 7150-7159, 2018.

[20] A. A. Lakshmi, C. S. Rao, M. Srikanth, K. Faisal, K. Fayaz, S. K. Singh, Prediction of mechanical properties of ASS 304 in superplastic region using artificial neural networks, *Materials Today: Proceedings,* Vol. 5, No. 2, pp. 3704-3712, 2018.

[21] S. Yaghoubi, F. Fereshteh-saniee, An Investigation on the Effects of Optimum Forming Parameters in Hydro-mechanical Deep Drawing Process Using the Genetic Algorithm, *Journal of Computational Applied Mechanics,* Vol. 49, No. 1, 2018.

[22] A. Sajadi, M. Ebrahimi, F. Djavanroodi, Experimental and numerical investigation of Al properties fabricated by CGP process, *Materials Science and Engineering: A,* Vol. 552, pp. 97-103, 2012.

[23] J. H. Holland, Adaptation in natural and artificial systems: an introductory analysis with applications to biology, control, and artificial intelligence, University of Michigan press Ann Arbor, 1975.

[24] K. Deb, Multi-Objective Optimization Using Evolutionary Algorithms. John Wiley& Sons, *Inc., New York, NY*, 2001.